

Improving SVM Classification Accuracy with Image Fusion-Based Gabor Texture Features

Kaynaştırılmış Görüntülerden Elde Edilen Gabor Doku Özellikleri ile DVM Sınıflandırma Performansının İyileştirilmesi

Cigdem Serifoglu Yilmaz^{1*}, Oguz Gungor¹

¹Karadeniz Technical University, Engineering Faculty, Department of Geomatics Engineering, 61080, Trabzon/Turkey.

ORIGINAL PAPER

*Corresponding author:

Cigdem Serifoglu Yilmaz
cigdemserifoglu@ktu.edu.tr

doi:

Article history:

Received : 04.02.2020

Accepted : 16.03.2020

Published: 31.03.2020

Abstract

Image fusion is one of the most common techniques used to enhance the interpretability and functionality of remotely sensed data. The aim of this study was to improve the performance of the SVM (Support Vector Machines) classifier with the aid of texture features (TF) extracted from fused images. As a first step, the spatial resolution of the WorldView-2 MS (multispectral) imagery was increased by fusing it with a WorldView-2 PAN (panchromatic) image using the PCA (Principal Component Analysis), WSB (Wavelet Single Band), GS (Gram-Schmidt), BRV (Brovey), EHL (Ehlers), HCS (Hyperspherical Colour Space), HPF (High-Pass Filtering) and MCV (Multiplicative) algorithms. A PCA transform was then applied on all fused images. The first principal component obtained from each fused image was used to extract the Gabor TFs. As a final step, extracted Gabor TFs were combined with the original MS image. Resultant images were classified with the SVM algorithm to investigate to what degree the used methodology affect the classification accuracy. The results showed that the GS fusion-based Gabor TFs provided the greatest classification accuracy increase with 19.3%, whereas the PCA fusion-based Gabor TFs resulted in the second best classification accuracy increase with 18.7%.

Keywords: Texture feature extraction, Image fusion, Gabor texture features, Principal component analysis, Image classification

Özet

Görüntü kaynaştırma, uzaktan algılanan verilerin yorumlanabilirliğini ve işlevselliğini artırmak için en yaygın olarak kullanılan tekniklerden biridir. Bu çalışmanın amacı Destek Vektör Makineleri (DVM) sınıflandırma algoritmasının performansının kaynaştırılmış görüntülerden elde edilen doku özellikleri yardımıyla iyileştirilmesidir. Bu amaçla, ilk aşama olarak bir WorldView-2 çok bantlı görüntüsü bir WorldView-2 pankromatik görüntüsü ile PCA (Principal Component Analysis), WSB (Wavelet Single Band), GS (Gram-Schmidt), BRV (Brovey), EHL (Ehlers), HCS (Hyperspherical Colour Space), HPF (High-Pass Filtering) ve MCV (Multiplicative) yöntemleri kullanılarak kaynaştırılmıştır. Daha sonra her bir kaynaştırılmış görüntüye Temel Bileşenler Analizi uygulanmıştır. Her bir kaynaştırılmış görüntü için elde edilen birinci temel bileşen Gabor doku özelliklerinin çıkartılması amacıyla kullanılmıştır. Son aşama olarak da elde edilen doku özellikleri girdi çok bantlı görüntüye eklenmiştir. Elde edilen bu görüntüler DVM algoritmasıyla sınıflandırılarak kullanılan metodolojinin sınıflandırma doğruluğunu ne derece etkilediği incelenmiştir. Sonuç olarak, GS yöntemiyle elde edilen Gabor doku özelliklerinin %19.3 artış ile sınıflandırma doğruluğunu en fazla oranda arttıran doku özelliği olduğu ve PCA yöntemiyle elde edilen Gabor doku özelliklerinin ise %18.7 artış ile sınıflandırma doğruluğunu en fazla oranda arttıran ikinci doku özelliği olduğu tespit edilmiştir.

Anahtar kelimeler: Doku özellik çıkarımı, Görüntü kaynaştırma, Gabor doku özellikleri, Temel bileşenler analizi, Görüntü sınıflandırma

1. Introduction

Image classification, which is one of the most widely-used techniques that increases the interpretability of the features on the image, categorizes image pixels with respect to their spectral features, i.e. spectrally similar pixels are assigned to the same class. Image classification is implemented for a wide range of purposes, including land use classification (Johnsson, 1994), geological mapping (Ricchetti, 2000), burned area mapping (Gitas et al., 2004), mapping crops and forest areas (Zabala et al., 2006), weed detection in crops (Eddy et al., 2006), imaging urban areas (Omkar et al., 2007), marine habitat mapping (Laurer and Aswani, 2008), crop identification (Yang et al., 2011), flood hazard assessment (Shaker et al., 2012), ocean mapping (Almendros-Jiménez et al., 2012), mapping riparian vegetation habitats (Kollár et al., 2013), land cover mapping (Damodaran and Nidamanuri, 2014), detection of land cover changes (Dube et al., 2014), mapping agricultural tillage practices (Ran et al., 2015), rice lodging assessment (Yang et al., 2017), and point cloud filtering (Yilmaz et al., 2018).

Image classification is a complex task and its success depends on several factors. Since bad atmospheric conditions and sensor malfunctions may affect the quality of the satellite imageries, atmospheric and radiometric corrections should be conducted to the imageries prior to classification, if necessary. Another important factor that plays a significant role in the success of a classification process is the experience of the analyst, especially when conducting supervised image classification that relies on the training pixels (signatures) collected by the analyst. Improper collection of signatures may lead to the confusion of the classes in the classified image. Spatial resolution of the image to be classified also affects the performance of the classification procedure employed. Since lower-resolution imageries are hard to interpret by the human eye, it may be very hard to collect signatures on this kind of imageries. Image fusion may provide an efficient solution to this problem. Since image fusion aims to produce spatially enhanced images by combining the spatial detail content of a panchromatic (PAN) image with the colour features of a lower-resolution multispectral (MS) image, it increases the interpretability of the images and makes it a lot easier to collect signatures for classification. The success of a classification process depends also on the spectral resolution (i.e. the ability to record the electromagnetic energy in a large number of spectral bands with narrow spectral band intervals) of the image to be classified. Images of higher spectral resolution are more effective in distinguishing land cover features, especially features with similar colour characteristics. On the other hand, classification of lower spectral resolution images requires some additional procedures to improve their classification performances. In this context, incorporating texture information to the classification process is a reasonable approach to enhance the performance of classification methods.

Until today, a great deal of effort has been made to use the texture features in image classification process to achieve better classification results. Baraldi and Parmiggiani (1995) incorporated six (energy, contrast, variance, correlation, entropy and inverse difference moment) of the Grey Level Cooccurrence Matrix (GLCM) texture features introduced by Haralick et al. (1973) into the classification process. Kurosu et al. (2001), Rao et al. (2002), Podest and Saatchi (2002), Butusov (2003), Sambodo et al. (2010), Hermosilla et al. (2010), Pathak and Dikshit (2010), Devi and Rekha (2013), Nanni et al. (2013) and Yilmaz (2019) are just some of the other studies where the use of GLCM texture features was investigated to achieve more accurate classification results. Augusteijn et al. (1995) performed image classification by using the texture features extracted from cooccurrence matrices, texture-tone analysis, grey level differences, Fourier spectrum and Gabor filters. Chen et al. 1997, incorporated the intensity and texture information into the classification process. In the study, the authors employed a wavelet transform to extract the fractal dimensions as texture features. Low et al. (1999) made use of texture features average intensity, second moment of intensity histogram and fractal surface dimension in an artificial neural network classifier. Nyongui et al. (2002) improved the classification accuracy by using texture features derived from first-, second-, and third-order statistics in spatial domain, texture features obtained from the texture spectrum, and texture features obtained from the grey level difference vector. Angelo and Haertel (2003) utilized the Gabor texture features in supervised image classification. Lloyd et al. (2004) indicated that the texture features extracted from variograms could be useful in increasing the classification accuracy. Zhang et al. (2004) increased the classification accuracy by using grey level cooccurrence texture features derived with geostatistical analysis. Jin et al. (2012) increased the classification accuracy by using multi-temporal texture features. Akar and Güngör (2015) integrated the GLCM and Gabor texture features into the random forest classifier to improve its performance. Yilmaz (2019) enhanced the performance of the support vector machines (SVM) classifier by using the GLCM texture features extracted from image segments obtained from fused images.

This study aimed to increase the SVM classification accuracy by integrating the Gabor texture features extracted from fused images. To this aim, the Gabor texture features derived from the results of various popular image fusion methods were integrated into the SVM classifier to see which fusion method provided the texture features that led to the greatest overall classification accuracy increase.

The remainder of this paper is as follows: Section 2 will give brief theoretical background for the image fusion methods used in this study. Section 3 will give information about the Gabor feature extraction process, whereas Section 4 will briefly explain the SVM classifier. Section 5 will introduce the study area and the methodology followed in this study.

The results regarding which fusion methods achieved the best texture features leading to the greatest classification accuracy increase will be given in Section 6. Finally, the conclusions drawn from this study will be given in Section 7.

2. Image Fusion

Image fusion combines the spatial characteristics of a high-resolution PAN band and colour features of low-resolution MS bands to produce spatially enhanced images. Fused images increase the interpretability of the images, enabling the users to extract meaningful information from the surface of the earth. Fused images have a wide variety of application areas, including topographic map updating (Pohl, 1996), RGB representation (Tsagaris and Anastassopoulos, 2005), building database updating (Poulain et al., 2011), visual display (Peli et al., 1999), land cover change detection (Zeng et al., 2010), marine monitoring (Du et al., 2003), mapping (Acerbi-Junior et al., 2006), flood plain mapping (Kedzierski et al., 2014), coastal monitoring (Yang et al., 2012), vegetation monitoring (Johnson et al., 2013) etc. A large number of image fusion approaches have been developed so far. Following are some brief information about the theories of the image fusion methods used in this study.

- The MCV method, which is the simplest of all, performs fusion by multiplying the input PAN and MS bands (Crippen, 1989). The BRV method calculates an intensity band by summing all MS bands. The ratio between each MS band and intensity band is multiplied by the PAN image to produce the fused bands (Hallada and Cox, 1983).
- The HPF method injects the spatial details enhanced by a high-pass filter into the MS image (Schowengerdt, 1980).
- The PCA method applies a PCA transformation of the input MS bands to de-correlate the image bands. The first principal component, which includes the majority of the total variance (i.e. spatial information), is then replaced by the input PAN image. The fused image is obtained through an inverse PCA transformation (Chavez and Kwarteng, 1989). The GS method, a statistical method like the PCA, combines the MS bands with a PAN band simulated from the MS bands, simulated PAN being the first band. A GS transformation is applied on this combined data. Then, the first GS component is replaced by the histogram-matched PAN band. An inverse GS transformation results in the fused image (Laben and Brower, 2000).
- The EHL method applies a high-pass filter on the panchromatic spectrum obtained from the Fast Fourier Transform (FFT) of the PAN image and a low-pass filter on the intensity spectrum obtained from the FFT of the intensity component generated through the IHS transformation of the MS bands. An inverse FFT is applied on both filtered spectrums and the results are summed to form a new intensity. Finally, an inverse IHS transformation with the new intensity results in the fused image (Ehlers, 2004; Klonus and Ehlers, 2007).
- The HCS method first simulates a smoothed PAN image and transforms the input data from native colour space to hyperspherical colour space. The intensity of the MS image is matched to those of the squares of the original and smoothed PAN image. Then, a new intensity component is generated using the squares of smoothed PAN, original PAN and MS intensity. Finally, an inverse transform is employed to produce the fused image (Padwick et al., 2010).
- The WSB method generates an approximation band from successive Discrete Wavelet Transformations (DWT). The generated approximation band is replaced by the input PAN image. An inverse DWT gives the fused bands (Hill et al., 2002; Yilmaz and Gungor, 2016; ERDAS IMAGINE Field Guide 2013).

3. Gabor Texture Feature Extraction

Texture information increases the meaningfulness of images. The Gabor filters, which are widely used to extract texture information from images, are a group of wavelets, each of them being able to acquire the energy at a given frequency and a given direction (Zhang et al., 2000). The Gabor filters provide optimal localization properties in both frequency and spatial domain, which makes them suitable for texture extraction (Yang et al., 2003; Huang et al., 2010). The Gabor transformation defines any signal as a summation of orthogonal frequency-shift and time-shift Gaussian functions. The Gabor space is obtained by convolving the image with a filter bank that includes various rotations and scales. Texture information is retrieved from the statistics of the filtering results (Akar and Güngör, 2015). The 2-D Gabor filter was given by Petkov and Wieling (2008) and Akar and Güngör (2015) as;

$$g_{\lambda, \theta, \varphi, \sigma, \gamma}(x, y) = \exp\left(-\frac{x'^2 + \gamma^2 y'^2}{2\sigma^2}\right) \cos\left(2\pi \frac{x'}{\lambda} + \varphi\right) \quad (1)$$

$$\begin{aligned} x' &= x \cos \theta + y \sin \theta \\ y' &= -x \sin \theta + y \cos \theta \end{aligned}$$

where, θ defines the orientation, λ is the wavelength of the filter, γ is the spatial aspect ratio and φ is the phase offset.

4. SVM Classification

The SVM method is based on the identification of decision boundaries, called hyperplanes, to optimize the boundaries between classes based on the sample pixels defined, thereby minimizing the possibility of misclassification between the pixels. The method was first designed to solve linear classification problems which can be labelled as $\{-1, +1\}$ to separate the two classes. In linear problems, the hyperplanes must have the highest level of aperture (i.e. margin) to effectively separate two classes. More specifically, the SVM method is based on the definition of the optimal hyperplane that maximizes the distance between the hyperplane and sample pixels (Vapnik 1995; 1998). Pixels on the optimal hyperplanes form support vectors and are used to classify the unknown pixels in the image (Özdarıcı Ok and Akyürek, 2013). Linear planes are often insufficient to solve real life problems. The concept of non-linear hyperplanes was developed for such cases. According to this concept, in order to ensure the best separation between classes, the data is transformed into the Euclidean space, also called multidimensional Hilbert space (Özdarıcı Ok and Akyürek, 2013). This transformation is done through the use of some kernel functions including the linear, polynomial, sigmoid and radial basis function kernels. These functions enable the transformation into a new higher dimensional space, where distinction between classes is more possible (Mathur and Foody, 2008). Among all, radial basis function is the most preferred one due to its efficiency in achieving high classification accuracy (Huang et al., 2002; Melgani and Bruzzone, 2004). Various multi-class approaches have been developed for cases where more than two classes should be separated. The One-Against-All approach forms an SVM for each class. Each SVM is trained to separate the samples of one class from the samples of all other classes (Milgram et al., 2006). On the other hand, the One-Against-One approach forms an SVM for each pair of classes. Let n be the number of classes in a problem, $n(n-1)/2$ SVMs are trained to separate the samples of a class from those of another (Milgram et al., 2006).

5. Application

5.1 Study Area

This study was conducted in the Surmene province of the city of Trabzon, Turkey. The study area was captured by the WorldView-2 satellite, which produces an 8-band MS image and a PAN image with spatial resolutions of 2 m and 0.5 m, respectively. The imageries produced by this satellite have a radiometric resolution of 11 bits. The location of the study area and Surmene province can be seen in Figure 1. As seen in the figure, the study area is a rural area covered by various types of vegetation and a certain amount of urban features.

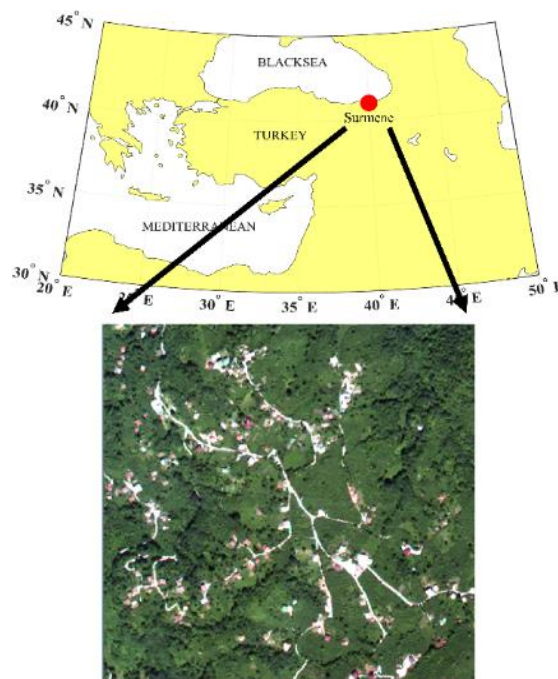


Figure 1. Study area

5.2 Methodology

Since the input images were atmospherically and radiometrically corrected, no preprocessing correction procedures were conducted before fusion. As the very first step, the spatial detail content of the WorldView-2 MS image was increased by fusing it with the WorldView-2 PAN image by means of the PCA, WSB, GS, BRV, EHL, HCS, HPF and MCV methods. The ERDAS IMAGINE software was used to apply all fusion methods except the GS, which was applied with a MATLAB script. All fusion methods were applied with default settings.

The next step was to apply a PCA transform on the fused images in order to de-correlate their bands. Since the first principal component of the transformed images contained the majority of the variance (i.e. spatial detail) of the fused bands, the Gabor TFs were extracted on them. The extracted TFs were combined with the original MS bands, which were upsampled to the size of the fused bands. When applying the Gabor transform, a scale of 5, a rotation of 8 and a window size of 39 were found to be efficient for texture features extraction. These parameter values were obtained by trial and error. It is important to note that, it was, of course, possible to extract the Gabor TFs from any PAN image without applying image fusion. However, the texture features are not only based on spatial features, but also on colour features. This is the reason that the TFs were extracted from the fused images in this study.

As the final step, the original MS image and the combined images were classified by the SVM method to investigate whether or not the followed procedure led to an increase in the classification accuracy, compared to the original MS image. The reason for using the SVM classifier in this study is because it has been proven to be one of the best classifiers in the literature (Bigdeli et al., 2012; Mathew and Anto, 2017). All images were classified into eight classes (i.e. tiled roof building, concrete roof building, road, soil, shadow, tea, hazelnut and tree) using the same signatures. The classification accuracy of each classified image was determined with respect to the reference control points that were randomly distributed over the study area. The actual class of each control point was identified by examining it on the high-resolution fused images. The overall classification accuracy of each classified image was calculated based on the number of the correctly classified control points. To conduct a robust classification performance evaluation, the number of the control points should be adequate to test the whole study area. This study used the multinomial distribution approach (Congalton and Green, 1999) to estimate the minimum number of control points required to compute the overall classification accuracy. This approach estimates the minimum number of required control points (N) as;

$$\begin{aligned} N &= \frac{S}{4b^2} \\ S &= a/k \end{aligned} \quad (2)$$

where, k is the total number of classes, a is the confidence interval and b is the desired accuracy. This study considered the confidence interval as 96%. Since each classified image consisted of 8 classes, S was computed as 0.005 ($S = 0.04/8$). χ^2 distribution table revealed that the probability level of 0.005 corresponds to 7.87 in one degree of freedom, hence, N was determined as 1229.7 ($7.87/(4 \times 0.04^2)$). Considering this, 2045 control points were decided to use to compute the classification accuracy of each classified image.

6. Results and Discussion

Figure 2 shows the images produced by the fusion methods used. As seen in the figure, all methods achieved to increase the spatial detail content to some degree. On the other hand, the WSB, GS and EHL methods produced images whose colour content was similar to that of the original MS image. The PCA, BRV, HCS and HPF methods presented moderate spectral consistency and the MCV method caused significant colour distortions, which can be seen in Figure 2.

The component substitution-based image fusion methods such as the BRV, PCA, GS and MCV are known for their success in enhancing the spatial detail quality. The MCV method injects the spatial details through the multiplication of the input MS bands by the input PAN band, which ensures a sharper image but increases the magnitudes of the pixel vectors after fusion, distorting the colour characteristics. The same is true for the BRV method, which sums all input MS bands to simulate an intensity component that is used to normalize the fusion results. The BRV method causes increases in the magnitudes of the pixel vectors, but not as much as the MCV does. This is why the BRV method achieved more realistic colours than the MCV method (see Figure 2).

The PCA method applies a PCA transform to the input MS image relying on the hypothesis that the first principal component of the transformed data includes the same amount of spatial detail content as the input PAN band. The first principal component is then replaced by the input PAN band. This procedure is successful in sharpening the images most of the time. But for some input MS images, it may produce blurry images or images with pixel block effects.

This happens when the first principal component does not include a reasonable amount of total variance (i.e. spatial detail content), which was the case in this study. It should be noted that the total amount of the variance contained in the first principal content varies from image to image.

For some input images, the first principal component contains almost all of the variance information, whereas less variance information may be contained in the first principal component of another images. If the input MS and PAN images are highly correlated, then the PCA method is expected to present a good performance in both spectral and spatial manner.

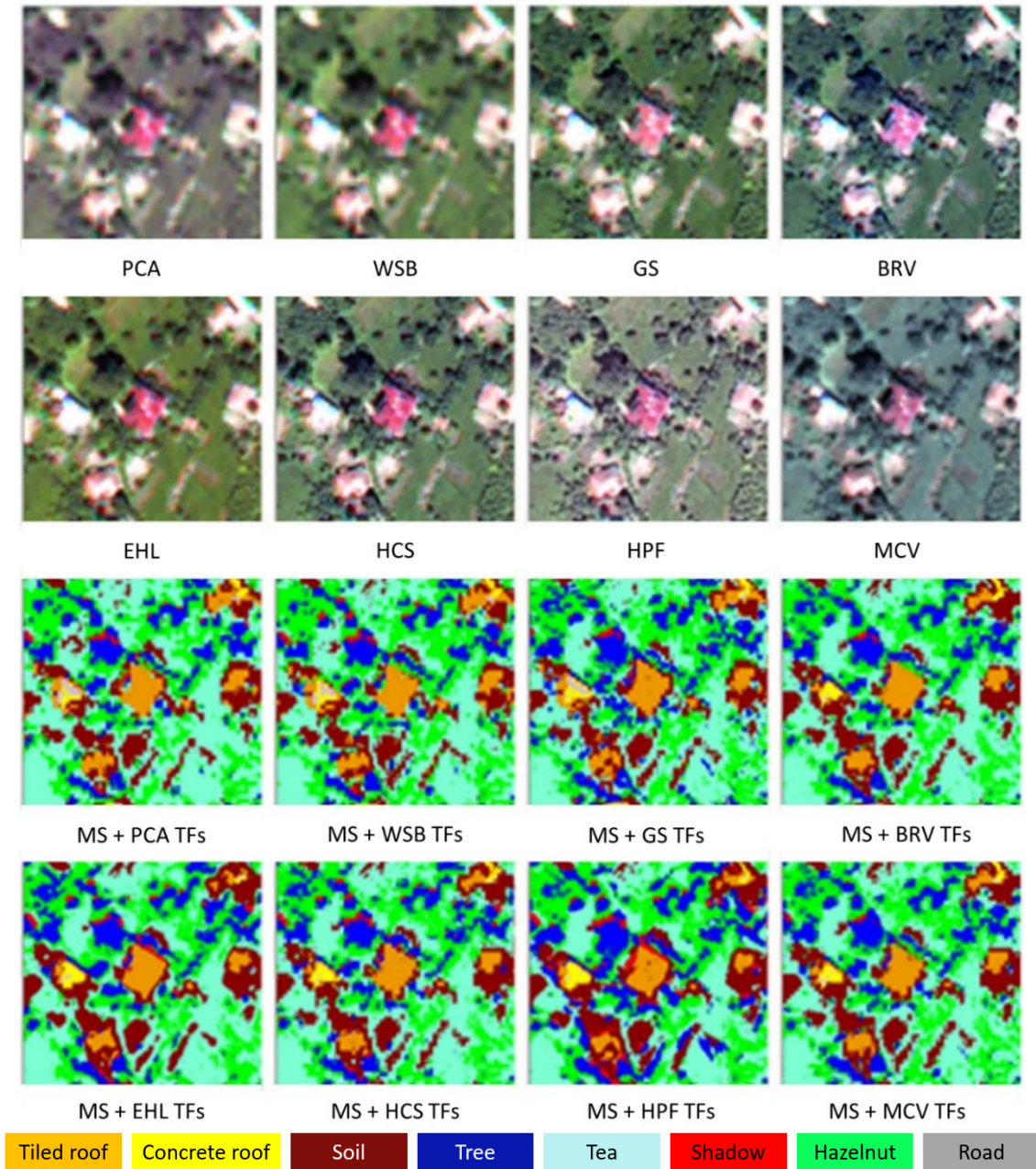


Figure 2. Classification accuracies of the original MS image combined with the image fusion-based TFs

The GS method is very similar to the PCA method. The difference between these two is that the GS method uses a lower resolution intensity image simulated from the input MS bands. The users may obtain the intensity band either by averaging the input MS bands or by linear combination of the input MS bands. It is also possible to define another lower resolution intensity image acquired from a different sensor. The success of the GS method depends on the statistical relationship between the lower resolution intensity image and input PAN band. If they have statistically similar characteristics, then the fusion result is expected to be spectrally and spatially more consistent.

This study used an intensity component obtained by averaging the input MS bands. Since the input images were acquired from the same sensor, the produced intensity component had similar statistics as the input PAN band. Also, the histogram matching applied between the intensity component and input PAN band ensured further resemblance between the statistical properties of both images. As seen in Figure 2, the GS method did not only preserved the colour features, but also injected the spatial details properly.

The EHL method applies a high-pass filter on the PAN spectrum and a low-pass filter on the intensity spectrum in the Fourier domain. This approach enabled the EHL method to better retain the colour features and enhance the spatial details of the PAN band. It is a well-known fact that, in most cases, filtering an image in the Fourier domain enables the extraction or enhancement of required features with less information loss, compared to the spatial domain. This was the case in this study. Hence, the new intensity component obtained by summing the inverse FFTs of both filtered spectrums helped transfer the spatial details without deteriorating the colour features of the input MS bands. The ERDAS IMAGINE software used to apply the EHL fusion method offers five window function for filtering in the Fourier domain; namely Ideal, Bartlett, Butterworth, Gaussian and Hanning. Our observations revealed that the Hanning filter achieved the best compromise between the colour and spatial detail quality of the fusion result. Hence this filter was used to filter the PAN and intensity spectrums in the Fourier domain. The ERDAS IMAGINE software allows the users to produce fused images with extreme colour or spatial detail quality. Since this study aimed to increase the SVM classification accuracy with the help of the Gabor texture features extracted from the fused images, both the spectral and spatial quality were important to us, therefore, we sought the best balance between the colour and spatial detail quality.

The WSB method applies DWT on the input PAN band until the spatial resolution of the input MS image is achieved. Each DWT results in four subbands (one approximation subband containing the colour information and three high frequency subbands containing the spatial content in horizontal, vertical and diagonal directions) with two times coarser spatial resolution. Since the spatial resolution of the input PAN band is four times better than that of the input MS image, two successive DWTs were applied on the input PAN band. These two DWTs caused a spatial detail loss to some degree. Another disadvantage of the DWT is that it extracts the spatial detail content in only horizontal, vertical and diagonal directions (Yilmaz et al., 2020), which led to a spatial detail loss in other directions in this study. As seen in Figure 2, the WSB method produced a blurry image despite its colour preservation success. Actually, this was expected because the multiresolution analysis based fusion methods have been proven to keep the colour content and deteriorate the spatial features (Gogineni and Chaturvedi, 2018; Serifoglu Yilmaz et al., 2019).

The HPF technique employs a high-pass filter on the input PAN image to enhance its spatial details. The ERDAS IMAGINE software used to implement this technique identifies the size and content of the high-pass filter with respect to the spatial resolution ratio (R) between the input images. Since the spatial resolution of the input PAN band was four times better than that of the input MS image, the software recommended to use a 9×9 high pass filter whose elements were set to -1 except the centre element, which was set to 80. The ERDAS IMAGINE software allows the users to define their own high-pass filters. Since, the efficiency of texture features has a strong relationship with the spatial detail quality of the image, we employed a 11×11 high pass filter on the input PAN band to further sharpen the fusion result at the expense of colour distortion, which can be observed in Figure 2. The HPF image, which is a function of R, is weighted relative to the global standard deviation of the MS bands (ERDAS IMAGINE Field Guide, 2013). The weight is calculated using the R and standard deviations of the filtered PAN band and input MS bands. This procedure enabled the crispness of the fusion result.

Table 1 shows the classification accuracies of the original MS image combined with the image fusion-based TFs. As seen in the table, all methods provided TFs that achieved to increase the classification accuracy.

Table 1. Classification accuracy of the classes

Data	Accuracy	Accuracy Increase
MS	77.6%	---
MS + PCA-extracted TFs	92.1%	18.7%
MS + WSB-extracted TFs	82.4%	6.2%
MS + GS-extracted TFs	92.6%	19.3%
MS + BRV-extracted TFs	89.0%	14.7%
MS + EHL-extracted TFs	87.8%	13.1%
MS + HCS-extracted TFs	87.6%	12.9%
MS + HPF-extracted TFs	89.4%	15.2%
MS + MCV-extracted TFs	79.4%	2.3%

As also seen in Table 1, combining the MS image with the GS- and PCA-based TFs increased the classification accuracy from 77.6% to 92.6% and from 77.6% to 92.1%, which led to an increase of 19.3% and 18.7%, respectively. The HPF and BRV were found to provide third and fourth best TFs. The TFs obtained from the WSB and MCV methods were found to lead to the smallest classification accuracy increase.

7. Conclusions

This study aimed to integrate the Gabor texture information extracted from the fused images into the SVM classifier to increase its performance. For this purpose, the PCA, WSB, GS, BRV, EHL, HCS, HPF and MCV fusion techniques were used to fuse a WorldView-2 MS image with a WorldView-2 PAN image. The first principal components of the PCA transformation of the fused images were used to extract the Gabor texture features. The extracted features were combined with the original MS image and the combined data were classified by the SVM algorithm. The results showed that all fusion techniques used yielded images that were useful to extract efficient Gabor texture features. The GS and PCA methods were found to provide the most efficient Gabor texture features, as they increased the SVM classification accuracy by 19.3% and 18.7%, respectively. On the other hand, the WSB and MCV methods yielded the texture features that led to the least classification accuracy increase. Future studies will focus on utilizing more advanced image fusion approaches to produce more efficient texture features, providing a greater classification performance.

References

- Acerbi-Junior, F. W., Clevers, J. G. P. W., & Schaepman, M. E. (2006). The assessment of multi-sensor image fusion using wavelet transforms for mapping the Brazilian Savanna. *International Journal of Applied Earth Observation and Geoinformation*, 8(4), 278-288. doi:10.1016/j.jag.2006.01.001.
- Akar, Ö. & Güngör, O. (2015). Integrating multiple texture methods and NDVI to the Random Forest classification algorithm to detect tea and hazelnut plantation areas in northeast Turkey. *International Journal of Remote Sensing*, 36(2), 442-464. doi:10.1080/01431161.2014.995276.
- Almendros-Jiménez, J. M., Domene, L., & Piedra-Fernandez, J. A. (2012). A framework for ocean satellite image classification based on ontologies. *IEEE Journal of selected topics in applied earth observations and remote sensing*, 6(2), 1048-1063. doi:10.1109/JSTARS.2012.2217479.
- Angelo, N. P., & Haertel, V. (2003). On the application of Gabor filtering in supervised image classification. *International Journal of Remote Sensing*, 24(10), 2167-2189. doi:10.1080/01431160210163146.
- Augusteijn, M. F., Clemens, L. E., & Shaw, K. A. (1995). Performance evaluation of texture measures for ground cover identification in satellite images by means of a neural network classifier. *IEEE Transactions on Geoscience and Remote Sensing*, 33(3), 616-626. doi:10.1109/36.387577.
- Baraldi, A., & Pannigiani, F. (1995). An investigation of the textural characteristics associated with gray level cooccurrence matrix statistical parameters. *IEEE Transactions on Geoscience and Remote Sensing*, 33(2), 293-304. doi:10.1109/TGRS.1995.8746010.
- Bigdeli, M., Vakilian, M., & Rahimpour, E. (2012). Transformer winding faults classification based on transfer function analysis by support vector machine. *IET Electric Power Applications*, 6(5), 268-276. doi:10.1049/iet-epa.2011.0232.
- Butusov, O. B. (2003). Textural classification of forest types from Landsat 7 imagery. *Mapping Sciences and Remote Sensing*, 40(2), 91-104. doi:10.2747/0749-3878.40.2.91.
- Chavez, A., & Kwarteng, P. (1989). Extracting spectral contrast in Landsat Thematic Mapper image data using selective principal component analysis. *Photogrammetric Engineering and Remote Sensing*, 55, 339-348.
- Chen, K. S., Yen, S. K., & Tsay, D. W. (1997). Neural classification of SPOT imagery through integration of intensity and fractal information. *International Journal of Remote Sensing*, 18(4), 763-783. doi:10.1080/014311697218746.
- Congalton, R. G., & Green, K. (1999). *Assessing the Accuracy of Remotely Sensed Data: Principles and Practices*. Boca Raton, FL: Lewis.
- Crippen, R. E. (1989). A simple spatial filtering routine for the cosmetic removal of scan-line noise from Landsat TM P-tape imagery. *Photogrammetric Engineering & Remote Sensing*, 55, 327-331.
- Damodaran, B. B., & Nidamanuri, R. R. (2014). Dynamic linear classifier system for hyperspectral image classification for land cover mapping. *IEEE Journal of Selected Topics in Applied Earth Observations and Remote Sensing*, 7(6), 2080-2093. doi:10.1109/JSTARS.2013.2294857.
- Devi, T. A. M., & Rekha, N. (2013). Hyperspectral Image Classification Using Spatial and Spectral Features. *International Journal of Scientific & Engineering Research*, 4(7), 1843-1847.

- Du, Y., Vachon, P. W., & Van der Sanden, J. J. (2003). Satellite image fusion with multiscale wavelet analysis for marine applications: preserving spatial information and minimizing artifacts (PSIMA). *Canadian Journal of Remote Sensing*, 29(1), 14-23. doi:10.5589/m02-079.
- Dube, T., Gumindoga, W., & Chawira, M. (2014). Detection of land cover changes around Lake Mutirikwi, Zimbabwe, based on traditional remote sensing image classification techniques. *African Journal of Aquatic Science*, 39(1), 89-95. doi:10.2989/16085914.2013.870068.
- Eddy, P., Smith, A., Hill, B., Peddle, D., Coburn, C., & Blackshaw, R. (2006, July). Comparison of neural network and maximum likelihood high resolution image classification for weed detection in crops: Applications in precision agriculture. In *2006 IEEE International Symposium on Geoscience and Remote Sensing* (pp. 116-119). IEEE. doi:10.1109/IGARSS.2006.35.
- Ehlers, M. (2004, October). Spectral characteristics preserving image fusion based on Fourier domain filtering. In *Remote sensing for environmental monitoring, GIS applications, and geology IV* (Vol. 5574, pp. 1-13). International Society for Optics and Photonics. doi: 10.1117/12.565160.
- ERDAS IMAGINE Field Guide 2013, Leica Geosystems, Atlanta, GA: ERDAS.
- Gitas, I. Z., Mitri, G. H., & Ventura, G. (2004). Object-based image classification for burned area mapping of Creus Cape, Spain, using NOAA-AVHRR imagery. *Remote Sensing of Environment*, 92(3), 409-413. doi: 10.1016/j.rse.2004.06.006.
- Gogineni, R., & Chaturvedi, A. (2018). Sparsity inspired pan-sharpening technique using multi-scale learned dictionary. *ISPRS journal of photogrammetry and remote sensing*, 146, 360-372. doi:10.1016/j.isprsjprs.2018.10.009.
- Hallada, W. A., & Cox, S. (1983, May). Image sharpening for mixed spatial and spectral resolution satellite systems. *Proceedings of the 17th International Symposium on Remote Sensing of Environment*, pp. 1023-1032, Ann Arbor, MI, USA.
- Haralick, R. M., Shanmugam, K., & Dinstein, I. H. (1973). Textural features for image classification. *IEEE Transactions on systems, man, and cybernetics*, (6), 610-621. doi: 10.1109/TSMC.1973.4309314.
- Hermosilla, T., Almonacid, J., Fernández-Sarría, A., Ruiz, L. A., & Recio, J. A. (2010). Combining features extracted from imagery and lidar data for object-oriented classification of forest areas. *International Archives of the Photogrammetry, Remote Sensing and Spatial Information Sciences*, 38, 194-200.
- Hill, P. R., Canagarajah, C. N., & Bull, D. R. (2002, September). Image Fusion Using Complex Wavelets. In *BMVC* (pp. 1-10).
- Huang, C., Davis, L. S., & Townshend, J. R. G. (2002). An assessment of support vector machines for land cover classification. *International Journal of Remote Sensing*, 23(4), 725-749. doi: 10.1080/01431160110040323.
- Huang, Z. C., Chan, P. P., Ng, W. W., & Yeung, D. S. (2010, July). Content-based image retrieval using color moment and Gabor texture feature. In *2010 International Conference on Machine Learning and Cybernetics* (Vol. 2, pp. 719-724). IEEE, Qingdao, China. doi: 10.1109/ICMLC.2010.5580566.
- Jin, H., Li, P., Cheng, T., & Song, B. (2012). Land cover classification using CHRIS/PROBA images and multi-temporal texture. *International Journal of Remote Sensing*, 33(1), 101-119. doi: 10.1080/01431161.2011.584077.
- Johnson, B. A., Tateishi, R., & Hoan, N. T. (2013). A hybrid pansharpening approach and multiscale object-based image analysis for mapping diseased pine and oak trees. *International Journal of Remote Sensing*, 34(20), 6969-6982. doi:10.1080/01431161.2013.810825.
- Johnsson, K. (1994). Segment-based land-use classification from SPOT satellite data. *Photogrammetric Engineering and Remote Sensing*, 60(1), 47-54.
- Kedzierski, M., Wilinska, M., Wierzbicki, D., Fryskowska, A., & Delis, P. (2014, May). Image data fusion for flood plain mapping. In *Proceedings of the 9th International Conference on Environmental Engineering, Vilnius, Lithuania* (pp. 22-23).
- Klonus, S., & Ehlers, M. (2007). Image fusion using the Ehlers spectral characteristics preservation algorithm. *GIScience & Remote Sensing*, 44(2), 93-116. doi: 10.2747/1548-1603.44.2.93.
- Kollár, S., Vekerdy, Z., & Márkus, B. (2013). Aerial image classification for the mapping of riparian vegetation habitats. *Acta Silvatica et Lignaria Hungarica*, 9(1), 119-133.
- Kurosu, T., Yokoyama, S., Fujita, M., & Chiba, K. (2001). Land use classification with textural analysis and the aggregation technique using multi-temporal JERS-1 L-band SAR images. *International Journal of Remote Sensing*, 22(4), 595-613. doi: 10.1080/01431160050505874.
- Laben, C. A., & Brower, B. V. (2000). Process for enhancing the spatial resolution of multispectral imagery using pan-sharpening. US Patent No. 6,011,875, filed 29 April 1998 and issued 4 January 2000 to the Eastman Kodak Company.
- Lauer, M., & Aswani, S. (2008). Integrating indigenous ecological knowledge and multi-spectral image classification for marine habitat mapping in Oceania. *Ocean & Coastal Management*, 51(6), 495-504. doi: 10.1016/j.ocecoaman.2008.04.006.

- Lloyd, C. D., Berberoglu, S., Curran, P. J., & Atkinson, P. M. (2004). A comparison of texture measures for the per-field classification of Mediterranean land cover. *International Journal of Remote Sensing*, 25(19), 3943-3965. doi: 10.1080/0143116042000192321.
- Low, H. K., Chuah, H. T., & Ewe, H. T. (1999). A Neural Network Landuse Classifier for SAR Images using Textural and Fractal Information. *Geocarto International*, 14(1), 66-73. doi: 10.1080/10106049908542096.
- Mathew, A. R., & Anto, P. B. (2017). Tumor detection and classification of MRI brain image using wavelet transform and SVM. In *IEEE 2017 International Conference on Signal Processing and Communication (ICSPC)*, pp. 75-78, Coimbatore, India. doi: 10.1109/CSPC.2017.8305810.
- Mathur, A., & Foody, G. M. (2008). Multiclass and binary SVM classification: Implications for training and classification users. *IEEE Geoscience and Remote Sensing Letters*, 5(2), 241-245. doi: 10.1109/LGRS.2008.915597.
- Melgani, F., & Bruzzone, L. (2004). Classification of hyperspectral remote sensing images with support vector machines. *IEEE Transactions on Geoscience and Remote Sensing*, 42(8), 1778-1790. doi: 10.1109/TGRS.2004.831865.
- Milgram, J., Cheriet, M., & Sabourin, R. (2006). "One against one" or "one against all": Which one is better for handwriting recognition with SVMs? *10th International Workshop on Frontiers in Handwriting Recognition*, Université de Rennes 1, La Baule, France.
- Nanni, L., Brahnam, S., Ghidoni, S., Menegatti, E., & Barrier, T. (2013). A comparison of methods for extracting information from the co-occurrence matrix for subcellular classification. *Expert Systems with Applications*, 40(18), 7457-7467. doi:10.1016/j.eswa.2013.07.047.
- Nyoungui, A. N., Tonye, E., & Akono, A. (2002). Evaluation of speckle filtering and texture analysis methods for land cover classification from SAR images. *International Journal of Remote Sensing*, 23(9), 1895-1925. doi:10.1080/01431160110036157.
- Omkar, S. N., Kumar, M. M., Mudigere, D., & Muley, D. (2007). Urban satellite image classification using biologically inspired techniques. In *IEEE International Symposium on Industrial Electronics* (pp. 1767-1772). doi:10.1109/ISIE.2007.4374873.
- Özdarıcı Ok, A., Akyürek, Z. (2013). Çok Tarihli Görüntü Sınıflandırmada Destek Vektör Makinaları ve Bulanık Mantık Yöntemi Kullanan Bölüt Tabanlı Bir Yaklaşım, *Türkiye Ulusal Fotogrametri ve Uzaktan Algılama Birliği VII. Teknik Sempozyumu (TUFUAB'2013)*, pp. 1-6, Trabzon, Türkiye.
- Padwick, C., Deskevich, M., Pacifici, F., & Smallwood, S. (2010, April). WorldView-2 pan-sharpening. In *Proceedings of the ASPRS 2010 Annual Conference*, San Diego, CA, USA, (Vol. 2630, pp. 1-14).
- Pathak, V., & Dikshit, O. (2010). A new approach for finding an appropriate combination of texture parameters for classification. *Geocarto International*, 25(4), 295-313. doi: 10.1080/10106040903576195.
- Peli, T., Peli, E., Ellis, K. K., & Stahl, R. (1999, March). Multispectral image fusion for visual display. In *Sensor Fusion: Architectures, Algorithms, and Applications III* (Vol. 3719, pp. 359-368). International Society for Optics and Photonics.
- Petkov, N., & Wieling, M. (2008). Gabor filter for image processing and computer vision. *On line*, <http://matlabserver.cs.rug.nl/edgedetectionweb/index.html>. Accessed on 18 February 2020.
- Podest, E., & Saatchi, S. (2002). Application of multiscale texture in classifying JERS-1 radar data over tropical vegetation. *International Journal of Remote Sensing*, 23(7), 1487-1506. doi: 10.1080/01431160110093000.
- Pohl, C. (1996). Geometric aspects of multisensor image fusion for topographic map updating in the humid tropics, PhD thesis, University of Twente.
- Poulain, V., Inglada, J., Spigai, M., Tournier, J. Y., & Marthon, P. (2011). High-Resolution Optical and SAR Image Fusion for Building Database Updating. *IEEE Transactions on Geoscience and Remote Sensing*, 49(8), 2900-2910. doi:10.1109/TGRS.2011.2113351.
- Ran, Q., Li, W., Du, Q., & Yang, C. (2015). Hyperspectral image classification for mapping agricultural tillage practices. *Journal of Applied Remote Sensing*, 9(1), 097298. doi:10.1117/1.JRS.9.097298.
- Rao, P. N., Sai, M. S., Sreenivas, K., Rao, M. K., Rao, B. R. M., Dwivedi, R. S., & Venkataratnam, L. (2002). Textural analysis of IRS-1D panchromatic data for land cover classification. *International Journal of Remote Sensing*, 23(17), 3327-3345. doi:10.1080/01431160110104665.
- Ricchetti, E. (2000). Multispectral satellite image and ancillary data integration for geological classification. *Photogrammetric Engineering and Remote Sensing*, 66(4), 429-435.
- Sambodo, K. A., Murni, A., & Kartasmita, M. (2010). Classification of polarimetric-SAR data with neural network using combined features extracted from scattering models and texture analysis. *International Journal of Remote Sensing and Earth Sciences*, 4(1), 1-17. doi:10.30536/j.ijreses.2007.v4.a1212.
- Schowengerdt, R. A. (1980). Reconstruction of multispatial, multispectral image data using spatial frequency content. *Photogrammetric Engineering and Remote Sensing*, 46(10), 1325-1334.

- Serifoglu Yilmaz, C., Yilmaz, V., Gungor, O., & Shan, J. (2019). Metaheuristic pansharpening based on symbiotic organisms search optimization. *ISPRS Journal of Photogrammetry and Remote Sensing*, 158, 167-187. doi:10.1016/j.isprsjprs.2019.10.014.
- Shaker, A., Yan, W. Y., & El-Ashmawy, N. (2012). Panchromatic satellite image classification for flood hazard assessment. *Journal of Applied Research and Technology*, 10(6), 902-911.
- Tsagaris, V., & Anastassopoulos, V. (2005). Multispectral image fusion for improved RGB representation based on perceptual attributes. *International Journal of Remote Sensing*, 26(15), 3241-3254. doi:10.1080/01431160500127609.
- Vapnik, V. (1995). *The Nature of Statistical Learning Theory*. New York, Springer-Verlag.
- Vapnik, V. (1998). *Statistical Learning Theory*. New York, Springer-John Wiley.
- Yang, B., Kim, M., & Madden, M. (2012). Assessing optimal image fusion methods for very high spatial resolution satellite images to support coastal monitoring. *GIScience & Remote Sensing*, 49(5), 687-710. doi:10.2747/1548-1603.49.5.687.
- Yang, C., Everitt, J. H., & Murden, D. (2011). Evaluating high resolution SPOT 5 satellite imagery for crop identification. *Computers and Electronics in Agriculture*, 75(2), 347-354. doi:10.1016/j.compag.2010.12.012.
- Yang, J., Liu, L., Jiang, T., & Fan, Y. (2003). A modified Gabor filter design method for fingerprint image enhancement. *Pattern Recognition Letters*, 24(12), 1805-1817. doi:10.1016/S0167-8655(03)00005-9.
- Yang, M. D., Huang, K. S., Kuo, Y. H., Tsai, H., & Lin, L. M. (2017). Spatial and spectral hybrid image classification for rice lodging assessment through UAV imagery. *Remote Sensing*, 9(6), 583. doi:10.3390/rs9060583.
- Yilmaz, V. (2019). Kaynaştırılmış Görüntülerden Elde Edilen Doku Özellikleri ile DVM Sınıflandırma Performansının İyileştirilmesi. *Geomatik*, 4(3), 190-200. doi: 10.29128/geomatik.507613.
- Yilmaz, V., & Gungor, O. (2016). Determining the optimum image fusion method for better interpretation of the surface of the Earth. *Norsk Geografisk Tidsskrift-Norwegian Journal of Geography*, 70(2), 69-81. doi:10.1080/00291951.2015.1126761.
- Yilmaz, V., Konakoglu, B., Serifoglu, C., Gungor, O., & Gökalp, E. (2018). Image classification-based ground filtering of point clouds extracted from UAV-based aerial photos. *Geocarto international*, 33(3), 310-320. doi:10.1080/10106049.2016.1250825.
- Yilmaz, V., Serifoglu Yilmaz, C., Güngör, O., & Shan, J. (2020). A genetic algorithm solution to the gram-schmidt image fusion. *International Journal of Remote Sensing*, 41(4), 1458-1485. doi:10.1080/01431161.2019.1667553.
- Zabala, A., Pons, X., Díaz-Delgado, R., García, F., Aulí-Llinàs, F., & Serra-Sagristà, J. (2006). Effects of JPEG and JPEG2000 lossy compression on remote sensing image classification for mapping crops and forest areas. In *IEEE International Symposium on Geoscience and Remote Sensing* (pp. 790-793). doi:10.1109/IGARSS.2006.203.
- Zeng, Y., Zhang, J., Van Genderen, J. L., & Zhang, Y. (2010). Image fusion for land cover change detection. *International Journal of Image and Data Fusion*, 1(2), 193-215. doi:10.1080/19479831003802832.
- Zhang, C., Franklin, S. E., & Wulder, M. A. (2004). Geostatistical and texture analysis of airborne-acquired images used in forest classification. *International Journal of Remote Sensing*, 25(4), 859-865. doi:10.1080/01431160310001618059.
- Zhang, D., Wong, A., Indrawan, M., & Lu, G. (2000). Content-based image retrieval using Gabor texture features. *IEEE Transactions PAMI*, 13-15.